Advances in Welding and Associated Inspection Technologies to Overcome Challenges in Clean Energy Sectors

T. Jayakumar
Metallurgy and Materials Group, Indira Gandhi Centre for Atomic Research, Kalpakkam 603 102
tjk@igcar.gov.in

1.0 INTRODUCTION

I consider it as a great honor for me and my colleagues at Metallurgy and Materials Group in Indira Gandhi Centre for Atomic Research (IGCAR) that I have been selected for this year's **Sir L. P. Mishra Memorial Lecture** by the Indian Institute of Welding (IIW-INDIA). Sir L. P. Mishra is a highly respected welding engineer who worked for Indian Railways and Hindustan Motors. He was the chairman of the first professional body (Indian Branch of Institute of Welding, London) of welding engineers in the country and he took initiative to transform this body into the Indian Institute of Welding, as we know today. It is a great privilege that I have been invited to deliver a lecture instituted in his honour. I also find the earlier recipients of this honour include eminent experts including Mr. M. N. Dastur, Mr. S. V. Nadkarni and Mr. P. S. Viswanath, to name a few. I thank IIW-INDIA with all humility for considering me one among these illustrious welding professionals.

As I personally believe that this honour is more a recognition to my colleagues in Metallurgy and Materials Group of IGCAR, I would like to dwell up on the contributions made by my team in the area of welding science and technology, with a special emphasis on India's Nuclear Programme. As most of you might know, at IGCAR, our main mandate is to conduct Research, Development and Design activities required for India's Sodium cooled Fast Reactor (SFR) programme, so that India will be self-sufficient in energy security by adopting this challenging technology. India's 500 Mwe Prototype Fast Breeder Reactor (PFBR), which is in the advanced stage of construction is a result of untiring efforts of hundreds of scientists, engineers and their colleagues at Kalpakkam. Many of us are closely associated with the development of advanced welding and hardfacing science and technologies to meet the challenging and highly demanding stringent requirements for the construction of the PFBR and associated fuel cycle facilities.

2.0 WELDING AND NDE TECHNOLOGIES FOR PFBR

2.1 End Plug Welding of Fuel Pins

2.1.1 Welding of IFAC-1 cladding tube with end plug

In tune with the mandate of IGCAR, let me start with welding technologies for PFBR. One of the important challenges in the fuel fabrication for PFBR has been the welding of fuel cladding tube with end plug. Welding is carried out in glove box as the fuel filled in the tube is radioactive. The weld joint should be of stringent quality, as the failure of the weld even after the removal of the fuel pin at its end of life is not acceptable. Such a failure would expose the highly radioactive spent fuel to primary sodium and may also interfere with fuel handling operations.

Fig. 1 shows the fuel pin, which consists of a cladding tube of 6.6 mm OD and a wall thickness of 0.45 mm and two solid end plugs. Choice of the material for cladding tube is based on its resistance to void swelling and at present 20% cold worked D9 alloy, an austenitic stainless steel with 15wt%.Cr, 15wt% Ni, 2wt% Mo and 0.4wt% Ti is used. Material for end plug is 316LN stainless steel. This materials combination is chosen because D9 alloy, exhibiting fully austenitic mode of solidification is prone to hot cracking. Both Gas Tungsten Arc Welding (GTAW) and Laser Welding (LW) procedures for welding cladding tubes and end plugs made from this materials combination have been successfully established. Fabrication of fuel pins for the first core of PFBR is in progress.

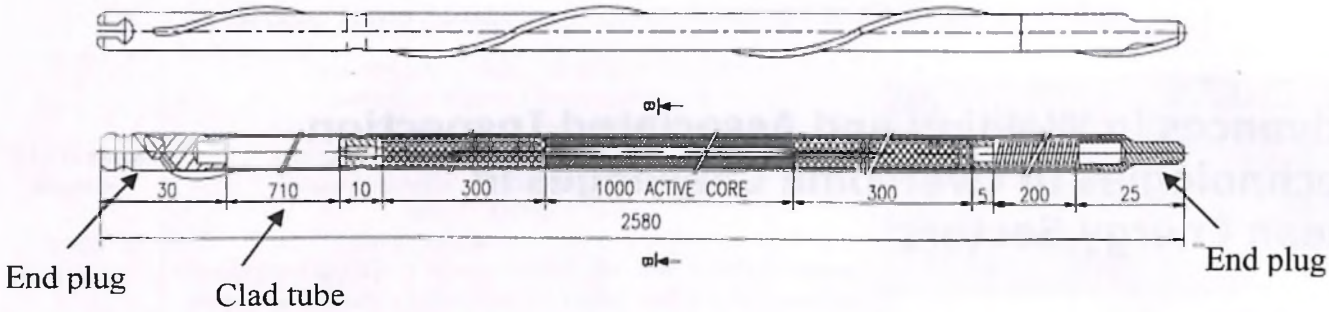

Fig. 1 : Fuel pin for PFBR

However, with an objective of improving the radiation swelling resistance of the clad tube and thus extend the life of the fuel pin and thus improve the amount of energy that can be extracted from the fuel inside it before it is taken out for reprocessing, IGCAR, in collaboration with MIDHANI has developed a new alloy, IFAC-1 (Indian Fast reactor Advanced Cladding-1), by modifying the composition of alloy D9 by increasing P and Si. Higher Si and P contents in IFAC-1 enhance the swelling resistance but make this alloy highly susceptible to hot cracking. Hence, a new procedure has to be developed for end plug welding of cladding tube made with the IFAC-1 alloy. **Table 1** gives the composition of IFAC-1 and 316LN stainless steel, the end plug material. **Fig. 2** shows the position of these alloys in Suutala diagram [1] which is widely used to assess the susceptibility of various austenitic stainless steels for hot cracking.

Extensive welding trials carried out with varied geometrical and process parameters for welding of the IFAC-1-SS and 316LN end plug to successfully obtain solidification crack-free welds. Weld cracks of varied lengths and widths were observed during the initial trials, before optimization of the procedure, as shown in **Fig. 3**.

During welding, the weld torch was focused towards the end plug side so that the weld metal contained more of 316LN SS and thereby increasing the Cr_{eq}/Ni_{eq} ratio. The end plug configuration was modified with a step of width of 0.5 mm on the end plug adjacent to the line of welding, as shown in **Fig. 4**.

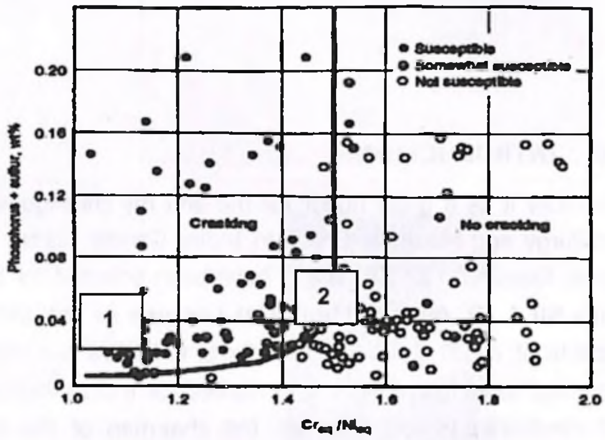

Fig. 2 : Relationship between solidification cracking susceptibility and Cr_{eq}/Ni_{eq} ratio

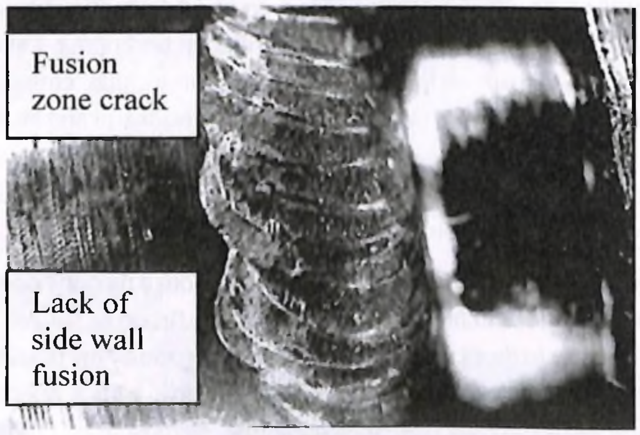

Fig. 3 : Welds with cracks during initial trials

Table 1 : Composition of IFAC-1 and SS 316 LN austenitic Stainless Steel

Material	P	Si	Ti	Ni	Cr	Mn	Mo	C	N	B	S	Fe
IFAC-1	0.04	0.75	0.25	15.38	14.35	2.36	2.40	0.046	0.01	0.0050	0.0046	Bal
]SS3161LN	0.03	0.5	0.05	12-12.5	17-18	1.6-2.0	2.3-2.7	0.024-0.030	0.06-0.08	0.002	0.01	Bal

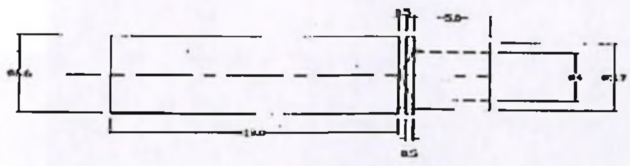

Fig. 4 : Modified end-plug configuration

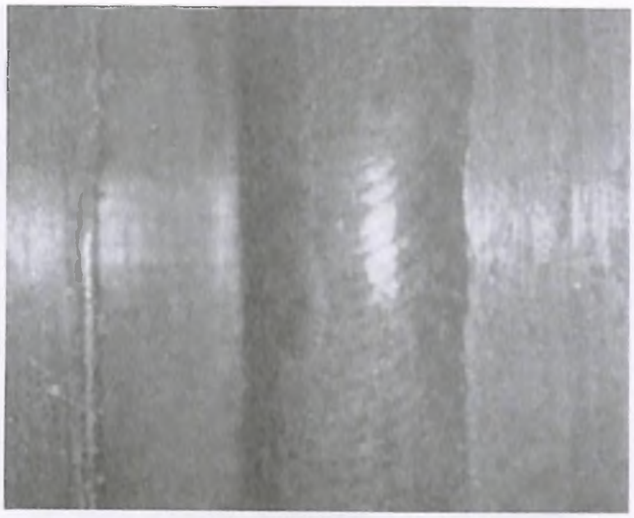

Fig. 5 : Defect-free weld

This step was helpful in achieving proper dilution of IFAC-1SS with SS 316LN in the molten pool.

By systematically varying the weld parameters such as peak current, background current, pulse width, pulse rate, weld speed, arc gap, electrode tilt, gas flow rate, and total time of welding during the trials, the number of cracks and their dimensions were gradually brought down and finally completely eliminated. Nearly 45 trial welds were carried out. Metallurgically defect-free welds of IFAC1-SS316LN qualified in leak testing and radiography have been produced (**Fig. 5**) in these trials and the optimum weld parameters have been established [2]. This experimental work gives us confidence that defect-free welds of IFAC-1SS-SS316LN can be produced.

2.1.2 Welding of Grade 91 Steel Cladding tube

The core of PFBR will use mixed oxide as the fuel. However, in future SFRs, metallic fuel (U-Pu-Zr alloy) will be used as fuel. For this fuel, cladding tubes and end plugs will be made from modified 9Cr-1Mo steel. Welding procedure has also been developed for fabrication of fuel pins using these tubes and end plugs. Though procedure adopted is same as the TIG welding employed for D9 alloy fuel pins, significant difference in the thermal conductivity of the ferritic steel and austenitic stainless steel and mandatory requirement for post weld heat treatments (PWHT) of the welds called for a separate procedure development for fuel pin fabrication of metallic fuel. Two welding machines, one for welding the top end plug outside the glove box and another for welding inside the glove box were qualified for welding these fuel pins by making 25 fuel pins of acceptable quality and these machines were used to fabricate the Nat. U-Zr fuel pins which are now undergoing irradiation studies in Fast Breeder Test Reactor for their qualification. **Fig. 6** shows the radiography image of one of such metallic fuel pins containing fuel and welded at both the ends.

2.2 Development of Activated-TIG Welding Technology

IGCAR has recently developed Activated Tungsten Inert Gas (A-TIG) welding technology for welding of both austenitic stainless steels. In this welding process, a thin layer of flux is applied on the weld location and this significantly improves the weld penetration so that plates or pipes of several mm thick can be welded autogenously by TIG processes in single pass without filler addition. This method of welding offers many advantages over conventional TIG welds, like no need for filler addition, no need for edge preparation etc., and hence immense potential for reducing the cost as well as time of fabrication. IGCAR holds international patent for this process and the technology has been transferred to Indian Industry for commercial production of this flux.[3]

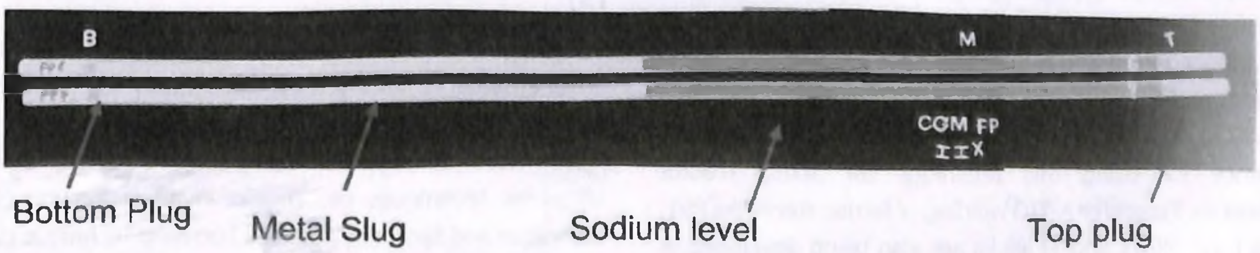

Fig. 6 : Radiography image of metallic fuel pins containing fuel and sodium made using modified 9Cr-I Mo steel clad tube and end plug

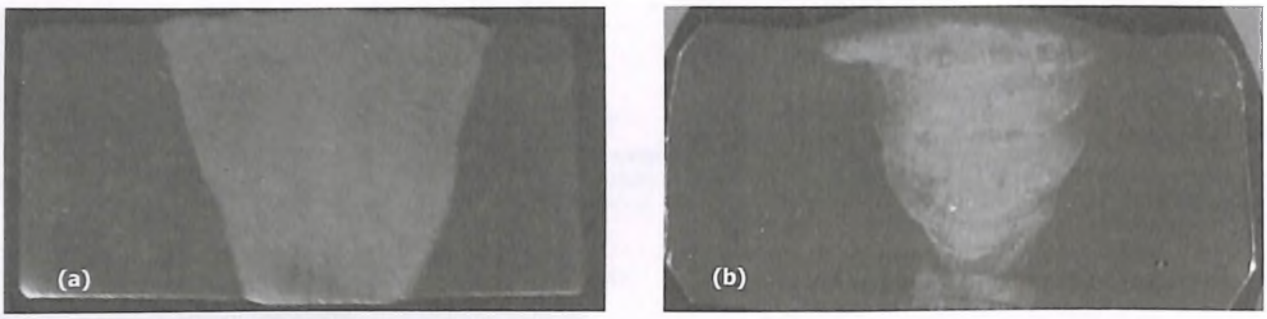

Fig. 7 : Macrograph of 10 mm thick austenitic stainless steel (a) A-TIG and (b) conventional TIG

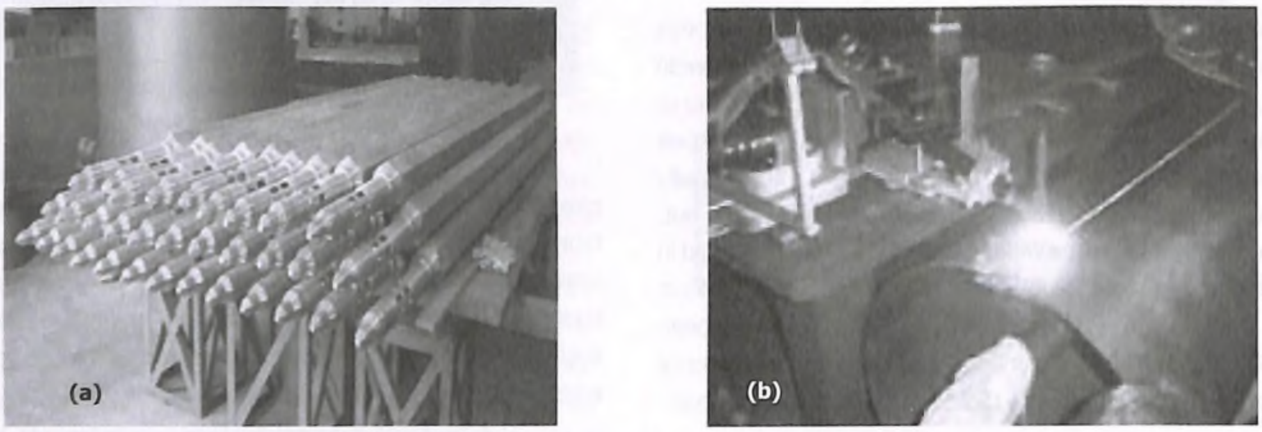

Fig. 8 : (a) Dummy fuel subassemblies fabricated by A-TIG process and (b) L-seam pipe welding in progress using A-TIG welding process

Fig. 7 shows the macrograph of A-TIG and conventional welds made using 10 mm thick austenitic stainless steel plates. Weld joints of austenitic stainless steels made by A-TIG welding process have been tested for various mechanical properties and corrosion resistance and it has been shown that the properties are either similar or better than that of the conventional TIG welds. It is also found that tensile residual stress in the weld zone is considerably less in A-TIG welds compared to conventional TIG welds [4].

IGCAR has fabricated several stainless steel components using A-TIG welding process which include several numbers of hexagonal tubes required for dummy fuel sub-assemblies (**Fig. 8a**) and pipe sections (**Fig.8b**) for reprocessing applications. It is planned to propose this technique for secondary sodium piping fabrication in the future sodium cooled fast reactors. Long term performance evaluation of the pipe joints fabricated using A-TIG welding process is being taken up to generate confidence for using this technique for actual reactor components. Fluxes for A-TIG welding of ferritic steels like P91, P92, Ni base alloys and Ti alloys are also being developed at IGCAR.

2.3 Development of Advanced Non-Destructive Evaluation (NDE) Techniques for Inspection of Welded Components

One of the mandates of my group in IGCAR is to develop advanced NDE techniques so that they can be used (a) as an alternative to conventional NDE techniques with specific advantages, (b) to comprehensively characterize materials and (c) for in-service-inspection of the reactor components. Many of these techniques have been used for inspection of the welded components. Some of these are briefly described here:

2.3.1 Ultrasonic TOFD and SAFT for Evaluation of Flaws in Weldments - An Alternative to Radiography [5]

In order to assess the usefulness of the ultrasonic technique as an alternative to widely used radiography for inspection of welds during fabrication, a systematic comparative study has been made among the radiographic and two advanced ultrasonic techniques i.e. Time-of-Flight Diffraction (TOFD) technique and Synthetic Aperture Focusing Technique (SAFT). The studies were carried out on a 18 mm thick carbon steel

weld pad with natural defects introduced at predetermined locations, as shown in the radiograph (**Fig.9**).

The TOFD technique is based on diffraction of ultrasonic waves at tips of discontinuities instead of geometrical reflections from the interface of the discontinuities. As TOFD technique relies solely on the time separation between signals diffracted from the edges of the defects, it can be performed almost independent of amplitude response and thus the coupling quality, material attenuation and defect orientation, and hence these variables are much less critical than with conventional pulse-echo methods.

SAFT is a signal processing tool that aims at improving the accuracy of ultrasonic signals, thus leading to better sizing capabilities. SAFT synthesizes a large focused transducer by gathering data at various positions using a small unfocused transducer. A synthetic aperture focusing system will produce a narrow synthetic beam by means of a coherent summation of phase adjusted pulses (A-scans), which results in greatly improved lateral resolution and the signal-to-noise ratio of the raw B-scan. The SAFT based reconstruction provides detailed information about the spatial location and extent of flaw contained in the inspected object.

The systematic studies carried out indicated that the TOFD technique could detect most of the defects, however it was not possible to clearly resolve and characterize the cluster of pores and group of cracks. Cracks with cleft edges were almost impossible to be identified. The experimental results revealed that TOFD technique, as a minimum, meets the codal requirements for detection of flaws. Sizing of length and through-wall extent can be carried out using the initial TOFD data as shown in **Fig.10**. However, it is found that the TOFD technique has serious limitation with respect to identifying defects close to scanning surface (top 6 mm) due to the merging of lateral wave with diffracted waves from defects. By employing SAFT, it is possible to resolve and characterize all the defects on-par or even better in comparison to the radiographic information. In addition, two clusters of porosity were distinctly seen which were separated by 7 mm apart and below 9 mm from the scanning surface, as shown in **Fig. 11**, demonstrating the superior spatial resolution as well as depth resolution of the technique. The SAFT has also provided better detection and characterization of oriented cracks which were missed by radiography. **Fig.12** shows the SAFT image corresponding to defects (P and Q) which were missed by radiography, whose presence were later confirmed by destructive tests as shown in **Fig. 13**. Hence, the inspection criteria of ASME code can be satisfied using ultrasonic imaging techniques such as TOFD and SAFT for detection, sizing and characterization of flaws in weldments, in lieu of Radiography.

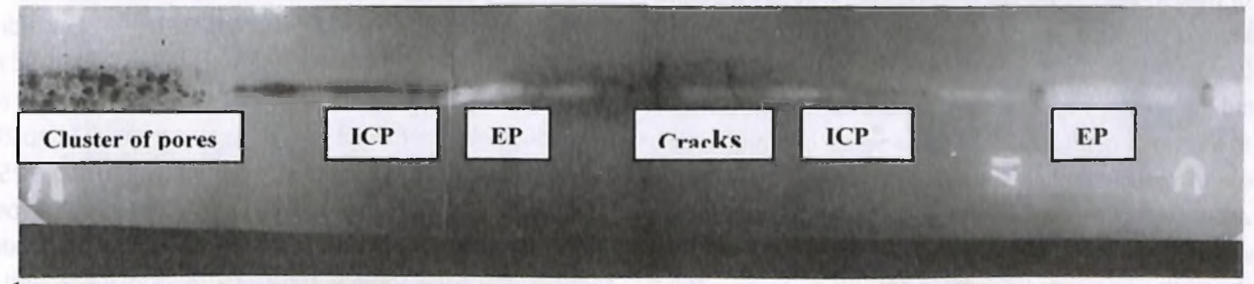

330 mm (12.99 in.)

Fig. 9 : Radiograph showing planar location of different defects in the weld pad ICP (Incomplete penetration), EP (-Excess Penetration)

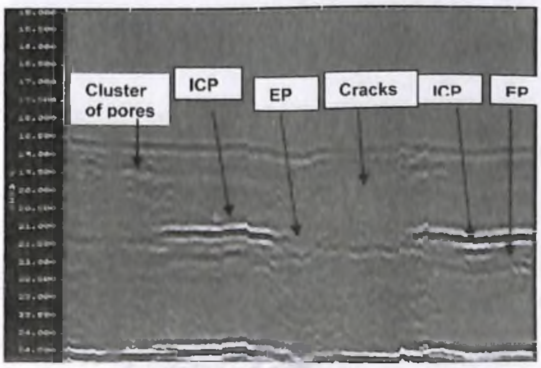

Scanning co-ordinate, mm

Fig. 10 : TOFD image for different defects in weld pad

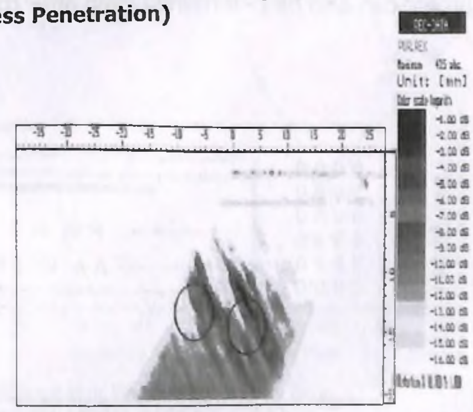

Fig. 11 : SAFT image showing two clusters of porosity separated by 7 mm apart 9 mm below scanning surface

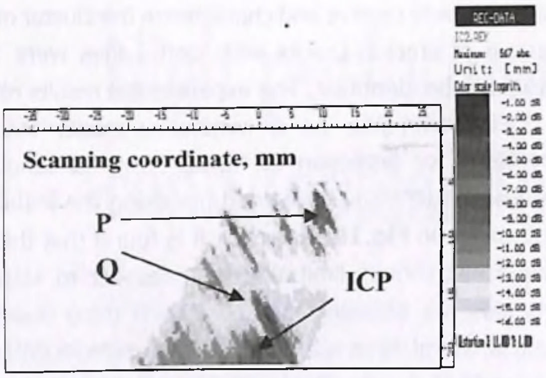

Fig. 12 : SAFT image showing ICP with an additional defect missed by radiograph

2.3.2 Imaging of weldments and assessment of PWHT

Ultrasonic velocity measurements have been carried out to get the weld profile and to assess the adequacy of PWHT in modified 9Cr-1Mo ferritic steel weldments [6]. Ultrasonic velocity measurements across the weld in the as-welded condition revealed that ultrasonic velocity is maximum in the parent metal and minimum in the weld metal (**Fig. 14**). As the amount of weld metal increased in the propagation direction of ultrasonic beam, ultrasonic velocity decreased and hence the amount of weld metal and parent metal could be determined in the propagation direction of ultrasonic beam, which could be used in-turn to get the weld profile. The ultrasonic velocity plot was found to almost replicate the weld profile. The lower velocity in the weld metal is due to the presence of martensitic structure with lower ultrasonic velocity. After PWHT (1033 K for 1h), ultrasonic velocity in the weld metal is found to be slightly lower than that in parent metal but is higher than that in the weld metal in the as welded condition (**Fig. 14**). Hence, the adequacy of PWHT can be assessed using ultrasonic velocity. The weld profile can also be determined even after the PWHT condition.

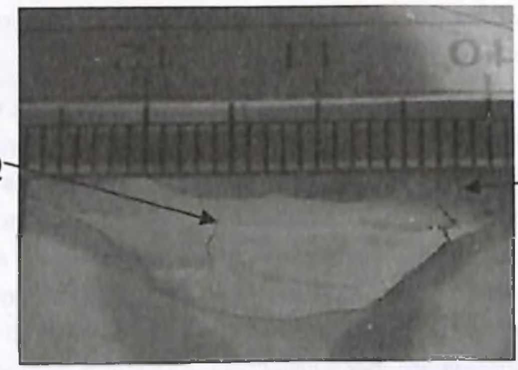

Fig. 13 : Image of defects missed by radiography but picked by SAFT

2.3.3 Ultrasonic imaging for early detection of Type-IV cracking in creep tested modified 9Cr-1Mo ferritic steel weldments [7]

Operational experience obtained from the usage of 9Cr-1Mo steel weldments at high temperature shows that failures in the weldments are due to type IV cracking which occur in intercritical/fine grained Heat Affected Zone (IC/FG HAZ). As the type IV damage initiates internally, its initiation cannot be detected using surface techniques such as in-situ metallography. Hence, ultrasonic imaging has been used in the present study for early detection of Type-IV cracking in creep tested modified 9Cr-1Mo ferritic steel weldments.

In order to simulate type IV damage in the steel weldment, various rectangular cross sectional specimens with weld in the centre of the gauge region were subjected to creep tests at 923 K and 50 MPa for different time durations from 527 h to 2820 h (sample ruptured). Ultrasonic C-scan imaging using a 25 MHz immersion focused transducer has been carried out across the weld line in the creep tested specimens in two perpendicular sections of the weldments. Ultrasonic velocity was found to be the minimum in the weld region and increased in the HAZs to reach a maximum in the parent metal. Hence, the HAZs could

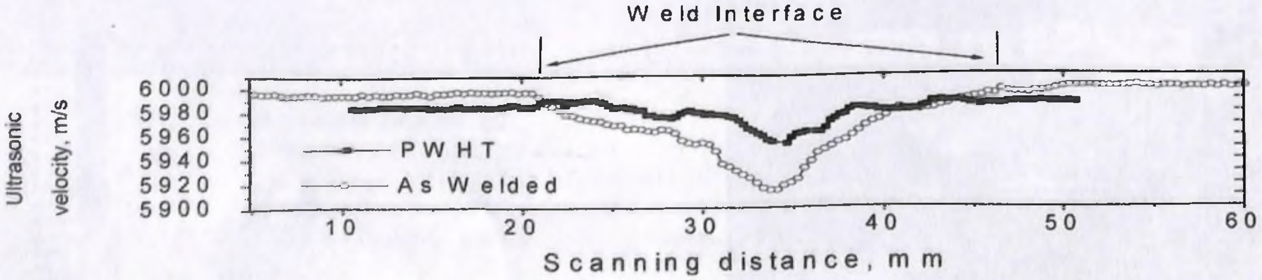

Fig. 14 : Variation in ultrasonic longitudinal wave velocity with scanning distance across the weld-line in as-welded and PWHT weldments

be differentiated from the weld and parent metals based on the velocity or in turn the time of arrival of the backwall echo. In the samples creep tested for durations up to 1011 h (~16 % failure strain), no localized damage could be detected. However, in the samples creep tested for more than 1992 h (~50 % failure strain), very high attenuation was observed in one or both sides of the welds in the HAZs (**Fig. 15**). The location of high attenuation was identified to be towards the parent metal i.e. in the intercritical / fine grained HAZ, typical of the type IV cracking. The study clearly demonstrated that ultrasonic measurements can be used for detection of the initiation of the type IV damage, when the damage is still confined internally and no change is observed on the surface.

2.3.4 Residual Stress Measurements in Welds of PFBR Main Vessel Sector

Ultrasonic non-destructive techniques are useful for the assessment of surface, sub-surface and bulk residual stresses. Critically reflected longitudinal wave (L_{CR}) transit time measurements have been carried out on AISI type 304 stainless steel weld joints in the PFBR main vessel mock-up sector in the longitudinal direction using carefully designed transducer-wedges, which generate and receive LCR waves. Austenitic stainless steel weld joint of the main vessel considered in this study is Single "V" and 35 mm thick weld joint. The transmitter-receiver assembly was moved over the weld centre and parent metal regions and residual stress measurements were taken in the direction parallel to the weld joint. Transit time measurements were made in steps of 2 mm as a function of distance from the weld centre. By using the predetermined value of the acoustoelastic constant (AEC) for AISI type 304 stainless steel, the residual stresses are obtained using the formula $V = V_o + A\sigma$, where V is the velocity in the presence of stress σ, V_o is the stress-free velocity and A is the AEC. Since the measurements were done with a fixed distance between the transmitter and the receiver, the velocity term can be replaced by the equivalent transit time in the above equation. Correspondingly, the AEC for the material and probe assembly combination has been obtained as 0.35 nsec/ MPa. **Fig. 16 (a)** shows the sector of the main vessel along with the weld in which the residual stress measurements are conducted and **Fig. 16 (b)** shows variation in residual stress across the weld region. It is seen from **Fig. 16 (b)** that maximum tensile residual stress occurs at the weld centre and the maximum compressive stress occurs around 25 mm away (heat affected

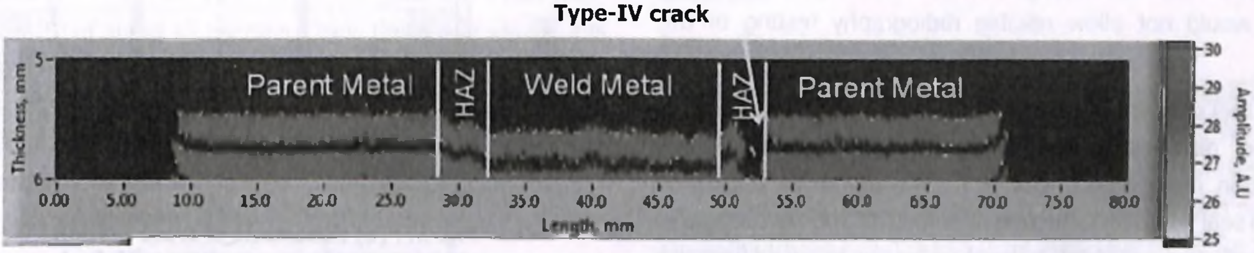

Fig. 15 : Ultrasonic b-scan image of the back wall echo across a ferritic steel weld subjected to creep at 923 K / 50 MPa for 1992 h.

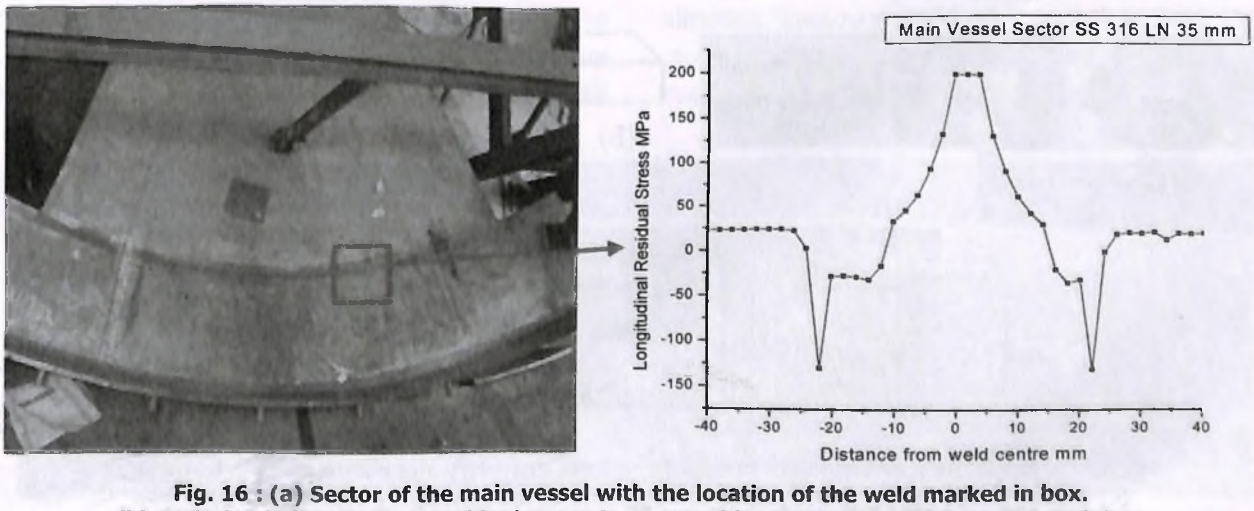

Fig. 16 : (a) Sector of the main vessel with the location of the weld marked in box. (b) Variation in longitudinal residual stress in 35 mm thick single "V" AISI type 304 stainless steel weld region as determined by the LCR wave transit time measurements.

zones) on either side of the weld regions. Quantitative estimation of the residual stresses also aids in optimization of the FEM based analysis for prediction of residual stresses and performance evaluation of welded components.

2.3.5 Development of Ultrasonic Guided Wave based Methodology for Inspection of Hexcan Seal Welds of PFBR Fuel Subassemblies

Fuel subassembly of a fast breeder reactor consists of a hexagonal wrapper tube (hexcan) which contains fuel pins. The hexcans of PFBR are 3600 mm long and made up of 3.2 mm thick cold worked austenitic stainless steel. The hexcan based fuel subassembly comprises of seal welds (**Fig.17a**), which join the 3.2 mm thick hexcan sheath to the thick head and foot sections of the subassembly. Structural integrity of the hexcan seal welds are very critical as any failure of these during service may result in separation of fuel pins from the bundles and consequent difficulties in discharging of fuel subassembly from the reactor core and/or failure of fuel pins leading to contamination of the sodium coolant with fuel and radioactive fission products. Hence, stringent quality control of hexcan seal welds becomes utmost important. The hexcan seal welds warranted development of a new methodology for inspection during the fabrication stage due to its complex geometry, which would not allow reliable radiography testing of the welds.

As the fuel subassemblies can not be immersed in water after the fuel pins are loaded, a contact guided wave based inspection methodology has been developed for testing of hexcan seal welds for detection of defects of 300 μm and more. The developed methodology involves testing the weld from the thinner plate side using 2.25 MHZ Rayleigh wave (**Fig. 17b**). This methodology is quite fast and can be used for detection of both axial and circumferential defects. This methodology has been employed on a hexcan weld having natural defects.

Fig. 17 (c) shows the B-scan image corresponding to one face of the hexcan having natural defects, as identified by the radiography. The defects could be identified by the presence of higher amplitude of the reflected signals. The sizes of the defects, as determined by this methodology, are found to be in close agreement with those obtained using the destructive in-situ metallography.

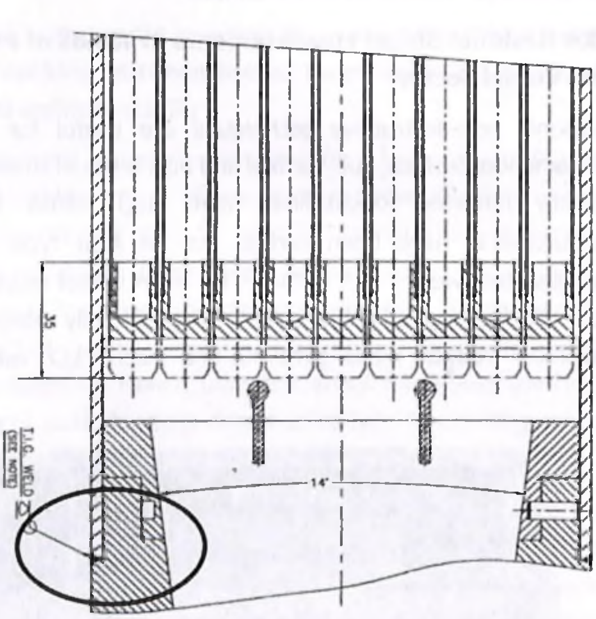

Fig. 17: (a) Schematic of cross section of hexagonal wrapper tube with fuel pins showing the seal weld location

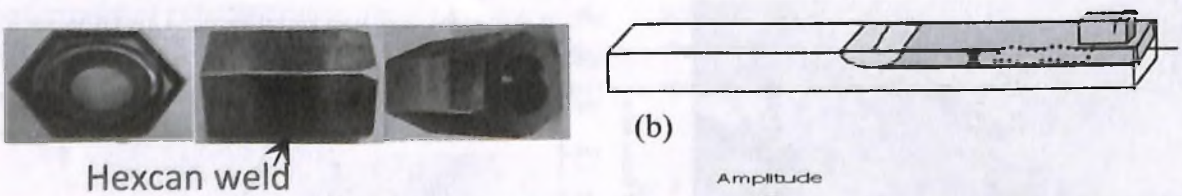

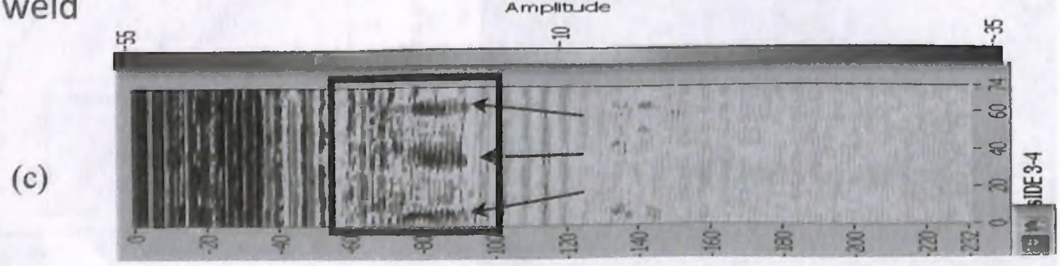

Fig. 17.(b) Actual Hexcan weld with schematic of joint geometry and position of the transducer (c) B-scan image based on the reflected amplitude of the Rayleigh wave. Rectangular box corresponds to the reflections from the weld region and higher amplitude (dark) signals corresponding to the defects are marked by arrows.

2.3.6 Microfocal Radiography of Tube to Tube Sheet (TTS) Weld Joints of Steam Generators of PFBR [8]

In the case of tube-to-tubesheet welds of steam generators of PFBR, due to the typical joint configuration, conventional ultrasonic testing and X-radiography are ruled out due to problems of access. Gamma radiography using a very small Thulium source (size 0.1 mm) or microfocal radiography using rod anode are the techniques which can be used for the detection of volumetric defects. In this case, we have used rod anode based micro focal radiography. The rod anode is inserted through the tube sheet side and positioned slightly offset with respect to the weld centre to ensure full coverage of the weld region. In the actual steam generator configuration, the maximum radial distance from the centre of one tube to the surrounding six tubes is 31.75 mm. This pitch distance limits the magnification for radiography to the maximum of 3. The microfocal radiography unit used for these investigations is of rod anode type (Fien Focus model 225 FXE) with a maximum voltage of 225 kV and current of 3000 μA. Due to the small inner diameter of the tube (12.6 mm), rod anode of length 350 mm and diameter 10 mm was selected. This rod anode had a flat target with X-rays being emitted with an emission angle of -5° x -55° x 360°. The microfocal X-ray unit used for the evaluation of TTS weld joints of steam generators had focal spot size (S) of about 15 microns. Using the above values, it is observed that the micro focal radiography technique is capable of detecting pores of the order of 27 microns or more as stipulated in the standards. **Fig.18** shows micro focal radiography image of a typical TTS weld joint which shows the micro-porosities, along with wire penetrameters.

2.4 Developments in NDE Techniques for In-Service Inspection

Objective assessment of the condition of structures, systems and components (SSCs) in order to carry out repairs or replacements at the most economic point in time, whilst still maintaining safety levels, is facilitated by in-service inspection (ISI) using NDE techniques. Depending upon the type of the component (in-core/out-of-core), NDE for ISI demands dedicated developmental research. For in-core components and systems, major challenges for ISI are limited access, high background radiation, high temperature, space restrictions and interference/disturbance from neighbouring components. All these put a greater demand to develop high sensitive, fast and automated NDE techniques armed with robotic devices, efficient sensors, advanced signal and image processing methods and knowledge based systems for in-service inspection of fast reactor components. Selection of NDE techniques for ISI is important as the sensitivity, capability, applicability and limitations of different techniques differ.

In the past two decades, extensive research has been carried out internationally to develop field worthy NDE methodologies with enhanced resolution for detection of in-service degradation in sodium cooled fast reactor components. Among these, most of the research activities have been focused on the inspection methodologies for critical components such as inspection of reactor vessel and steam generators of the reactors. In this section, the NDE methodologies developed in the author's laboratory for ISI of the reactor vessels are discussed.

2.4.1 ISI of Reactor Vessels

Main vessel (MV) of the PFBR contains the whole reactor assembly and is surrounded by the safety vessel (SV) with a gap of about 300 mm between the two vessels. ISI of MV and SV can be carried out through this gap only. Various sensors, instrumentation and robotics have been developed for the ISI of MV and SV to be carried out at a temperature of 150°C. ISI vehicle has been designed to carry the industrial CCTV camera, ultrasonic transducers and eddy current sensors. Ultrasonic methodologies have been developed for 100% volume inspection of the welds and the heat affected zones (HAZs) in

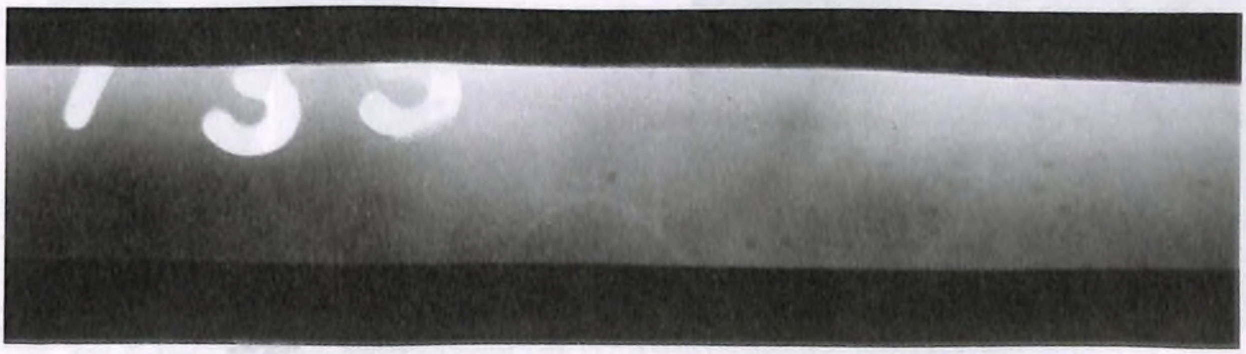

Fig. 18 : Microfocal radiography image of a typical TTS weld joint with micro-porosities.

the vessels using high temperature integral ultrasonic transducers having three probes of 0, 45 and 70 degree angles. The device would be capable of identifying all welds and carrying out visual and ultrasonic inspections.

2.4.1.1 Identification of Weld Centre Line using Eddy Current Technique [9]

Identification of weld centre line is necessary for fixing the required skip distance and scan ranges for ultrasonic testing of the welds. In the case of components made of austenitic stainless steels, by making use of the presence of ferromagnetic delta ferrite in the weld material, eddy current inspection can be employed for identification of weld centre line. For this application, high temperature ECT probe has been developed, which has been tested to work upto 200°C. **Fig.19a** and **Fig. 19b** show the scanning of the hot weld plate using high temperature ECT probe and the eddy current based image of the weldment respectively. Due to predominant variations in the electrical conductivity and magnetic permeability (due to the presence of delta ferrite), the weld region has been distinctly noticed in the eddy current images. The weld centerline could be determined with an accuracy of 0.5 mm.

2.4.2 ISI of the Shell Weld of the Core Support Structure [10]

In-service inspection of the shell weld of the core support structure (CSS) in the main vessel of PFBR is important and at the same time is challenging. Going beyond the inspection code requirements, an innovative ultrasonic inspection methodology has been developed for in-service inspection of the shell weld of the core support structure in the main vessel of PFBR. The inspection of this weld immersed in sodium required the development of a special methodology because of the restricted access to the weld, curvature of the main vessel and ultrasonic beam skewing that occurs at the K type weld used for joining the main vessel to the support shell plate. **Fig. 20a** shows the schematic of the test methodology along with the cross-sectional view of the core support structure showing the shell weld to be inspected. The inspection of the shell weld is carried out from the outside surface of the main vessel as indicated by arrow shown in **Fig. 20**, using normal beam ultrasonic transducer. Because of the presence of curvature in the main vessel, ultrasonic beam enters the weld overlay at an angle α to the support shell structure (**Fig. 20**). Further, because of the presence of columnar grains in the austenitic stainless steel weld overlay and the K weld, ultrasonic wave gets skewed and enters at an angle β to the support shell plate (**Fig. 20**). Beyond this point, ultrasonic wave propagates in the support shell structure at the angle β and gets reflected every time it encounters the plate surface. When the wave encounters any defect/interface in the shell plate, ultrasonic wave is reflected from the defect/interface and is picked up by the same transducer. By changing the location of the transducer, angles α and β get changed and hence a defect at any location and orientation in the core support structure can be detected/ evaluated, except at the locations hidden by the inlet pipes.

Fig : 19 (a) Scanning of the hot weld plate using high temperature ECT probe

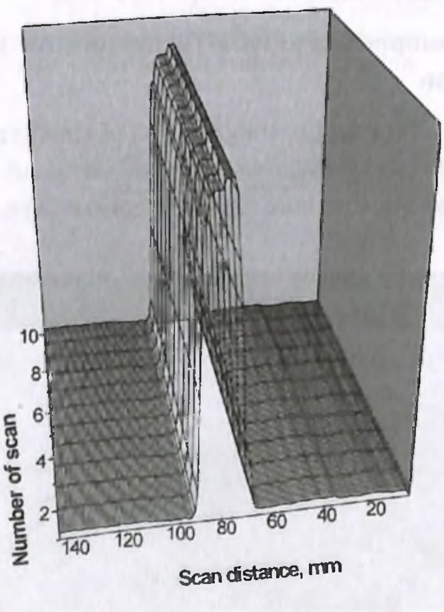

Fig : 19 (b) High temperature ECT based image of the weldment

The developed methodology has the advantage that inspection at multiple angles of ultrasonic wave propagation can be achieved just by moving a single normal beam ultrasonic transducer along the curved surface of the main vessel (A to B in **Fig. 20**). Multiple angle beam inspection would ensure the detectability of defects of any orientation. The time window in the beam path is selected suitably to analyze a defect in the shell weld region. The methodology has been successfully demonstrated on the main vessel sector using standard artificial defects. In order to simulate the defects in the shell weld of actual main vessel, a 30 mm thick stainless steel plate was welded at the top of the shell plate of the main vessel sector mock up using a K-type weld. Notches of dimensions 20% and 30 % of wall thickness, made in this weld have been successfully detected. **Fig. 20** shows a typical signal from a 9 mm deep (30% wall thickness) notch in the simulated shell weld of core support structure located at a distance of 450 mm from the outer surface of the main vessel. This is the first time worldwide that such a methodology has been developed for inspection of a critical weld, which was originally designed to be non-inspectable, thus enhancing the reliability and safety of the reactor system. The ultrasonic testing, using this methodology, indicated that a defect down to 20 % wall thickness (~ 6 mm) on both sides of the support shell plate and the shell weld can be detected reliably.

2.5 Non Destructive Evaluation for Metallurgical Characterisation of Welds

Procedures have been developed using various NDE techniques for metallurgical characterization of weld joints. Two of these developments, assessment of sensitization in austenitic stainless steel welds and assessment of crack closure during fatigue crack growth are described here.

2.5.1 Detection of Sensitization in Austenitic Stainless Steel Welds [11]

This work deals with assessment and quantification of sensitization in AISI Type 316L welds. Welded joints of AISI Type 316L stainless steel were aged at 973 K for periods of up to 200 h. The base and weld metal components of the aged joints were then assessed for susceptibility to sensitization and intergranular corrosion (IGC) by using various tests specified by ASTM A262, Practices A and E. The possibility of using eddy current testing (ECT) to detect sensitization and IGC was assessed. ASTM A262 Practice A and E tests indicated sensitization in base metal aged for 20 h and above. Aged weld metals showed no failure in these tests. The ECT technique was investigated in order to assess its suitability for the detection and quantification of sensitization. The ratio of eddy current amplitudes after and before exposure to $Cu–CuSO_4–H_2SO_4$ solution was used as an assessment criterion. A significant increase in this ratio was observed on aging the base metal for more than 20 h. Change observed in the ratios of eddy current amplitudes for weld metal is only marginal (**Fig. 21**). The ECT results correlated very well with the findings of the EPR and ASTM Practice E tests. This indicates that ECT holds promise as an on-line monitoring tool for sensitization and IGC.

2.5.2 SS 316(N) Welds: Assessment of Crack Closure Effects during Fatigue Crack Growth: Acoustic Emission Results [12]

Acoustic emission technique was used successfully in characterization of fatigue crack growth (FCG) behaviour of

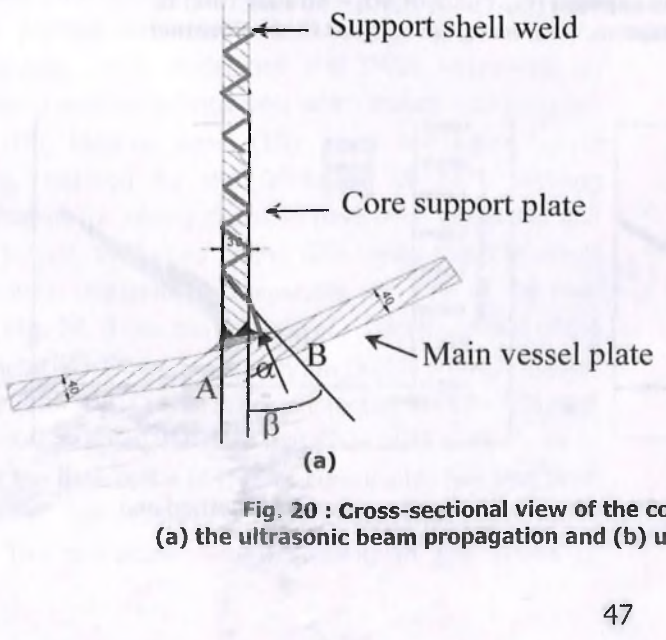

(a)

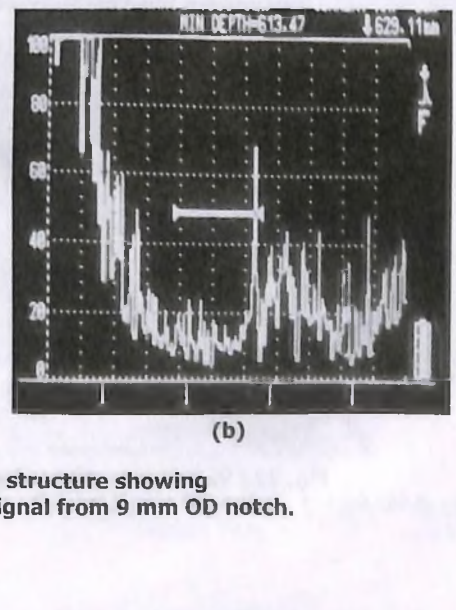

(b)

Fig. 20 : Cross-sectional view of the core support structure showing (a) the ultrasonic beam propagation and (b) ultrasonic signal from 9 mm OD notch.

welds, in a campaign to understand the effect of R ratio (K_{min}/K_{max}) on the FCG properties. FCG tests were done at different R values in the range 0.1 to 0.45. The FCG curves showed R dependence, especially in the threshold regime. Crack closure/opening loads were determined by (i) conventional method (deviation from linearity in load-CMOD plots, and by (ii) monitoring the AE signals simultaneously (the maximum RMS voltage – **Fig. 22**). AE method being more sensitive yields a higher value than that obtained for conventional methods. When closure correction is incorporated using these values, $\Delta P_{eff} = P_{max} - P_{op}$, the R-dependence vanishes. Thus using acoustic emission technique, it is possible to demonstrate that FCG behaviour is independent of R, by giving correction to closure effect.

3.0 INTELLIGENT WELDING [13]

With advances in information technology, it is possible to integrate welding power sources, automation and on-line monitoring into an Intelligent Welding System capable of adaptive control of welding parameters using the feedback from NDE sensors. A computer-controlled expert system would process signals received from NDE sensors during welding and offer on-line advice for taking corrective actions in the welding power source or weld carriage for affecting changes in the process parameters and thereby avoiding welding defects. Development of such an intelligent welding system which involve (i) NDE sensor(s) capable of on-line monitoring during welding with fast response for defect detection, (ii) an expert system software that can process signals from NDE sensor(s),

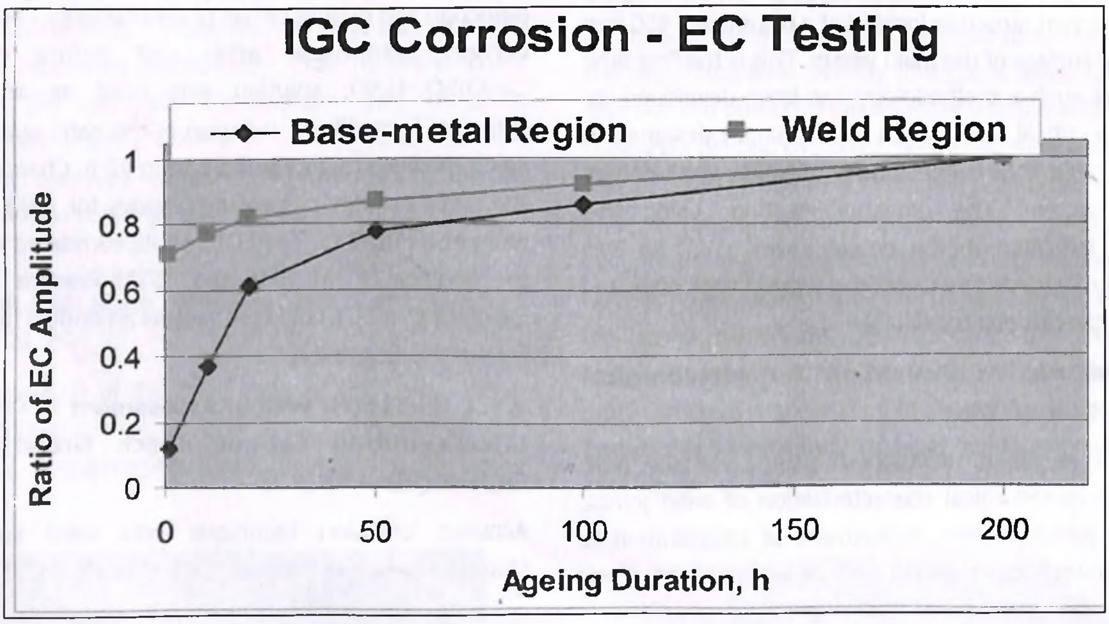

Fig. 21 : Ratio of EC amplitudes of aged exposed ($Cu-CuSO_4-H_2SO_4$ – Strauss Test) to unexposed Base metal prone to sensitization, weld metal is resistant to sensitization

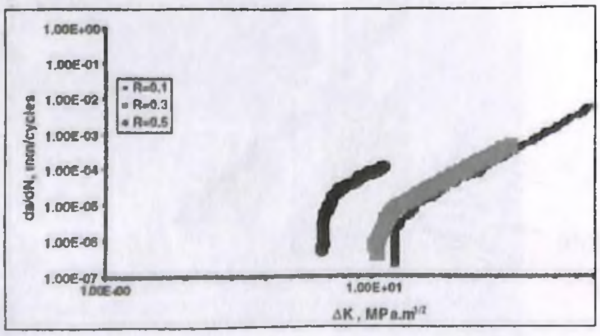

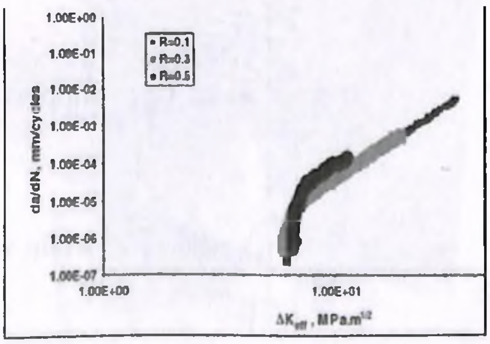

Fig. 22 : Variation in FCG behaviour with ΔP_{eff} estimated using a)conventional method and b) using acoustic emission data collected during FCG test.

identify defects, find out process variable(s) that cause the defects, and give corrective feedback to the welding power source or welding carriage/robot, and (iii) welding equipment and carriage/robot capable for responding to instructions from the expert system is under development at IGCAR. An infra red camera which can measure temperature distribution in the weld pool has been integrated with welding machine with feed back control (**Fig.23**). From the temperature data recorded by infrared imaging system, it is possible to predict width and depth of the weld bead (**Fig. 24**). With analysis of the temperature distribution, it is also possible to detect defect formation in the weld, which can in turn be used to alter the welding parameters suitably. The ultimate aim of such a system would be to obtain defect-free welds repeatedly in the first attempt. Once integrated with a welding robot, the system would be capable of automatic welding of different joint designs, thicknesses, etc. Such systems can also be used for remote welding, particularly for remote repair applications.

4.0 TECHNOLOGY DEVELOPMENT FOR FABRICATION OF INDIAN TEST BLANKET MODULE (TBM) FOR ITER

India is one of the countries associated with the development and testing of Test Blanket Module (TBM) in ITER. **Fig. 25** shows the schematic of important components of TBM which is approximately 1.66 m in height and 1.5 m in width and 0.57 m in depth. Material chosen for the construction of TBM is Reduced Activation Ferritic Martensitic Steel (RAFMS) which is essentially a 9Cr steel containing W and Ta as the major alloying elements and concentration of the impurity elements are controlled to minimize induced radioactivity from these elements, once the material is put in service in a fusion reactor. IGCAR working closely with Institute of Plasma Research, Gandhinagar, ARCI, Hyderabad and DRDL Hyderabad, in developing welding technologies, which include Gas Tungsten Arc (GTA), Electron Beam (EB), Laser and Laser Hybrid welding, required for the fabrication of TBM. Welding consumables for joining this steel have been developed and characterized. Properties of the GTA welds met the entire specification requirement comparable with that of the base metal. **Fig. 26**, shows the variation of impact toughness of the weld metal with temperature. Very low Ductile Brittle Transition Temperature (DBTT) is an important requirement for this steel and it may be noted that weld metal has DBTT comparable to that of the base metal [14]. This consumable has also been successfully used to carry out Hybrid laser welding of RAFM steel. The procedure for EB welding to join plates of

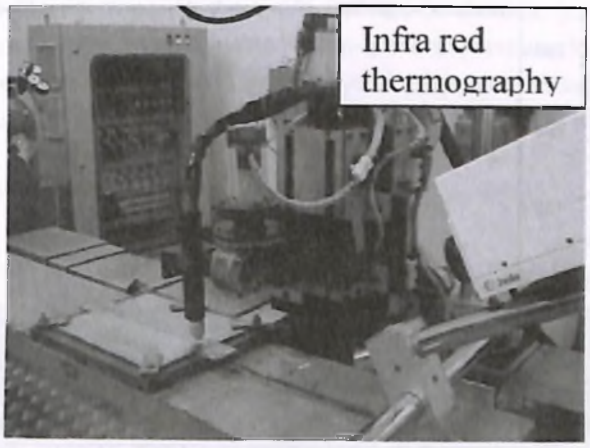

Fig. 23 : Intelligent welding set up at IGCAR

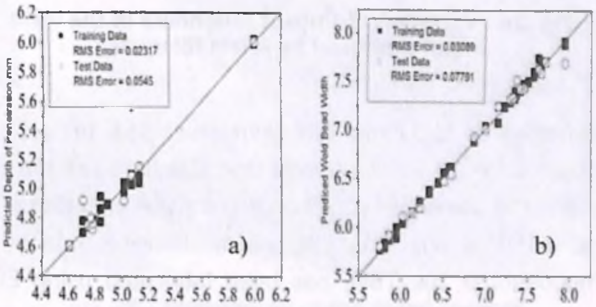

Fig. 24 : Comparison of predicted bead a) depth and b) width with measured values

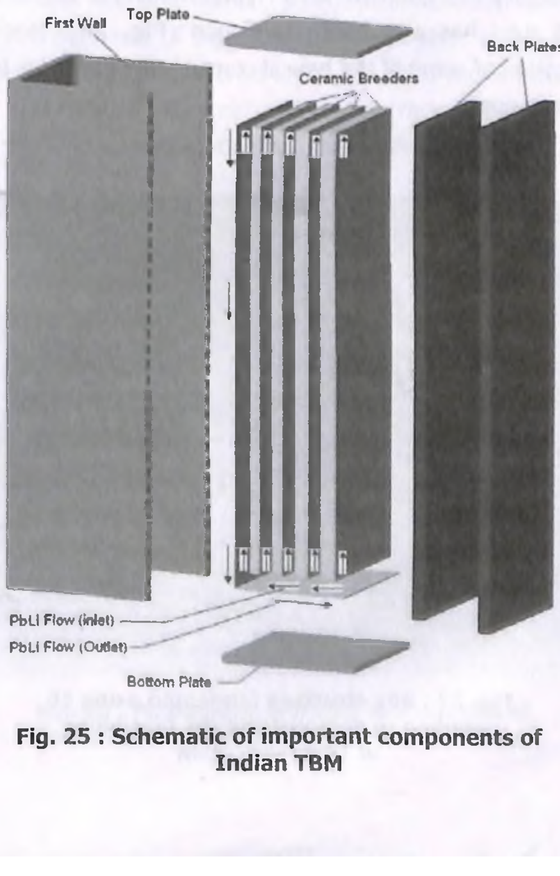

Fig. 25 : Schematic of important components of Indian TBM

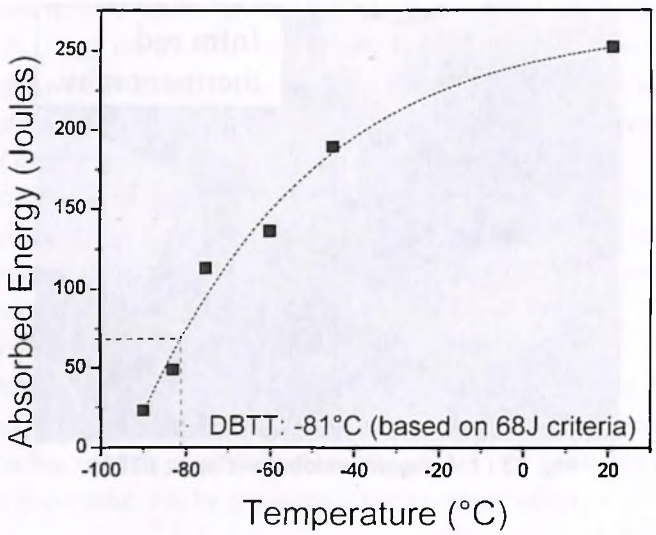

Fig. 26 : Variation of Impact toughness of the weld metal produced by RAFM filler wire

thicknesses up to 12 mm has been developed. Impact tests conducted on EB welds showed that toughness of the weld metal in the as-welded condition is comparable to that of the base metal. A box structure, which simulates one of the components of the TBM, has been fabricated using EB to demonstrate the applicability of the process for component fabrication (**Fig. 27**). Laser welding of 6 mm thick plates of RAFM steel has also been carried out successfully and the properties of the weld joints have been found to be satisfactory. Procedure for laser Hybrid welding of 12 mm thick RAFM steel has also been developed (**Fig. 28**). Mock up fabrication of some of the typical components of TBM is being taken up now.

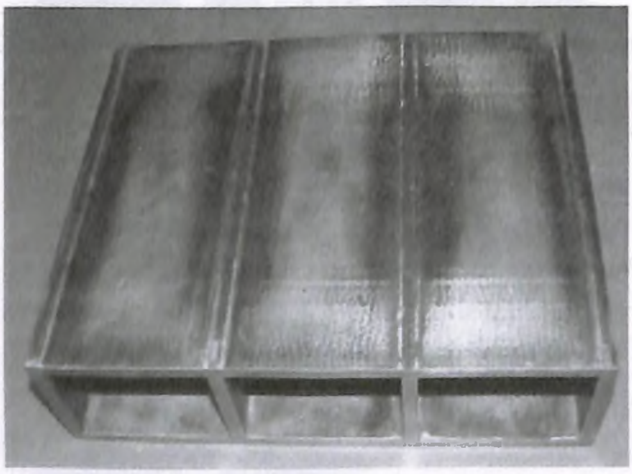

Fig. 27 : Box structure fabricated using EB welding to demonstrate the feasibility of TBM fabrication

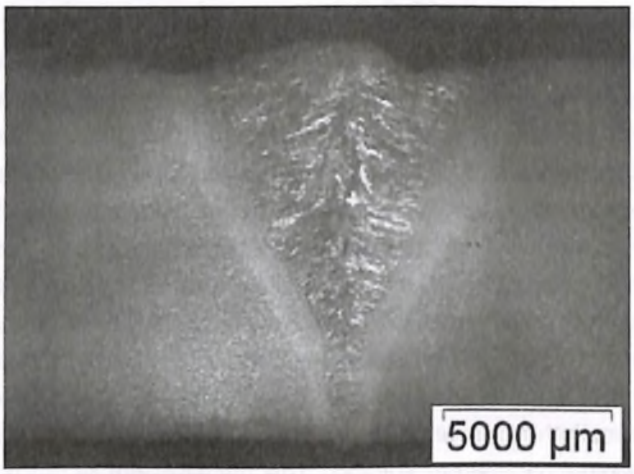

Fig. 28 : Macrostructure of laser hybrid weld produced using 12 mm thick RAFM steel

5.0 DEVELOPMENT OF WELDING TECHNOLOGIES FOR ADVANCED ULTRA SUPER CRITICAL THERMAL POWER PLANTS

IGCAR, along with BHEL and NTPC has taken up an ambitious project of development of indigenous technologies for Advanced Ultra Supercritical (AUSC) thermal power plants with an operating temperature of 700°C and pressure of 300 bars. In addition to materials that used in the fossil power plants that are in operation, there is need to develop advanced materials such as type 304HCu stainless steel (UNS S30432) and alloy 617M and their welding consumables for this application. Type 304HCu SS is a variant of conventional austenitic stainless steel grade of 18Cr-8Ni with addition of 3 wt % of copper, increased carbon content and controlled amounts of niobium and nitrogen which can be used in fossil power plants up to about 630°C. Alloy 617M is a Ni base alloy which can be used for temperature beyond 650°C up to 720°C. IGCAR in association with MIDHANI has successfully developed filler wires for joining of both 304HCu and Alloy 617M. Further, procedure for welding 304HCu SS tubes of 52 mm diameter with a wall thickness of 9.5 mm has been developed using three different filler wires of 304HCu, alloy 625 and alloy 617M. Weld defects like root crack, hot crack and crater cracks observed during the initial trials in weld joints made from nickel base filler wires due to sluggishness in fluidity of weld metal were overcome by suitably altering the weld joint design and optimisation of heat input. Subsequently welding procedures were finalised and the weld joints produced as per this procedures were qualified by liquid penetrant and radiography examinations. The weld joints also cleared the tensile and bend test as per ASME section IX requirements. Production weld joints made using this qualified procedures are being tested for long term mechanical properties like creep, fatigue, creep crack growth and fatigue crack growth.

6.0 FAILURE ANALYSIS OF WELDS

Contributions of Metallurgy and Materials Group in IGCAR towards welding science and technology include analyses of many weld failures for both for Dept. of Atomic Energy and outside agencies. Availability of expertise in welding metallurgy, in situ metallography, non-destructive testing, corrosion and mechanical property evaluation often made our group as one of the important destinations on issues related to weld failures. By systematic investigation covering design of the components, selection of materials, fabrication, choice of consumables and heat treatment, verification of the operating conditions and metallurgical investigations, it was possible to analyse the causes of failure and recommend remedial actions. Causes of failures included choice of wrong welding consumable, wrong heat treatment, defects in the welds, lack of proper inspection etc. One case study of the failure analysis is included here as an illustrative example.

6.1 Failure Analysis of Dissimilar Weld Joint of a Steam Pipeline Reducer [15]

A high pressure steam pipe line reducer commissioned in a fertilizer plant failed after a short period of 2200 hours. The failure occurred in the form of a big circumferential crack at the welded interface between the pipeline and the header. The material of construction of the reducer pipe was AISI A 335 P22 grade material conforming to 2.25 Cr- 1Mo ferritic steel with a wall thickness of 30 mm. This pipe is welded to AISI 347 type SS header. The reducer carries steam at a nominal pressure of 115 MPa and at a temperature of 788 K. To make the dissimilar joint, the edge of reducer was buttered with Inconel 82 for a length to 12mm. Post weld heat treatment was given for two hours at a temperature of 973-1013 after the buttering for the pipeline. This pipeline was welded to the stainless steel header using Inconel 82 (GTAW for root pass) and Inconel 182 (for SMAW process) consumables. The weld joint was not inspected using any non-destructive testing (NDT) techniques and also no post weld heat treatment (PWHT) was given to this joint after welding. The reducer, which was received for investigation had only the buttered layer and a portion of the weld. The failed component in the as received condition is shown in **Fig.29**. The circumferential length of the crack was found to be approximately 300mm. The crack was found to be just below the weld fusion line. Dye-penetrant examination was carried by applying the penetrant to the outside surface and the developer to the inside surface, to characterize the crack. The crack was found to be non-branching and was found to extend by another 50mm, beyond what was observed visually.

Fig. 29 : Photograph of the failed reducer

In-situ metallographic examination was carried out on the outside surface of the reducer, at a location where the crack terminated, in the ferritic steel/buttered interface. This revealed presence of cracks at the ferritic steel and buttered layer interface and buttered layer and weld metal interface. **Fig. 30** reveals a major circumferential crack observed at the interface and its propagation into the buttered layer.

Microhardness measurements taken across the buttered layer and ferritic steel interface showed that hardness of the alloy

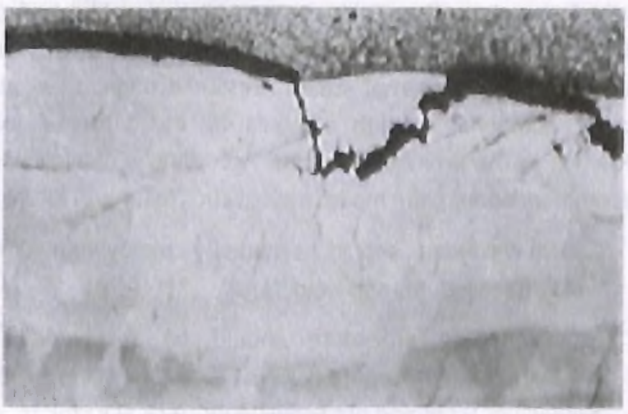

Fig. 30 : Photograph showing propagation of circumferential crack into the buttered layer

steel is around 230 VHN in the base material, 290 VHN at the heat affected zone, 360 VHN at the interface and 280 VHN at the buttered portion. Hardness at the interface between the buttered layer and ferritic steel interface is higher than what is expected in the HAZ of the ferritic steel after PWHT. Metallographic examination revealed presence of circumferential cracks between the ferritic steel and the buttered layer. Further, the cracks are penetrating into the buttered layers from the ferritic steel. There are many micro cracks and defects in the buttered layers, which indicate poor weld quality.

It is well known that transition metal joints between Cr-Mo ferritic steels and austenitic stainless steels are prone to cracking in service at the ferritic steel in the interface between the weld and ferritic steel and weld by propagation of low ductility circumferential cracks along a planar array of globular carbides. Even joints made using nickel base welds are not immune to failures and a number of premature failures are reported in service, in such joints. These cracks are due to various factors like (a) large difference in thermal expansion between austenitic stainless steel and ferric steels, which generate secondary stresses at the interface, (b) carbon migration from the ferritic steel side due to difference in carbon activity, resulting in the formation of precipitate rich high hardness zone at the interface, (c) notching effect caused by differences in the oxidation resistance of the ferritic steel and austenitic steel. The welding characteristics of Inconel/Nickel due to poor flow properties give rise to defects and d) thermal stresses at the interface due to startup-shutdown cycles also contribute to premature failures.

From the evidences obtained during the investigation, it is concluded that the failure of the weld interface was due to the improper buttering/welding and post weld heat treatment that resulted in low ductility circumferential cracks adjacent to the weld fusion line. The residual stress at the weld interface, stress generated during frequent startups/shut downs and variations in the internal steam pressures might have also added additional enough stresses at the buttered joint resulting in the premature failure. Accordingly, the following recommendations were made to avoid such failures in future:

- Critical weld joints should be made by employing qualified welding procedures and welders.
- Proper PWHT procedure should be followed. The recommended procedure is PWHT at 973 K ($^{+0}/_{-15}$) not exceeding 973K and not below 958K (973-15K) for 1h per 25 mm thickness.
- During buttering, increase the current, decrease the speed and increase the inter pass /pre heat temperature.
- Ultrasonic inspections to detect weld defects, at the weld interface.
- Use of trimetallic joints with Alloy 800 as a transition piece.

7.0 CONCLUDING REMARKS

In this Sir L. P. Mishra Memorial Lecture based paper, I have restricted myself to include only those welding research and development studies in which I have been actively involved. This is only a small part of what is going on in the area of welding in my group at IGCAR. My colleagues are actively involved in development of welding consumables, repair welding, hardfacing, evaluation of weldability of steels (hydrogen assisted cracking) and austenitic stainless steels (hot cracking). Extensive mechanical and metallurgical characterization of weld joints is also going on among various Divisions of my group. Further, some of my colleagues are actively associated with the Indian Institute of Welding in its effort to project Indian Welding Science and Technology in International Forums. They represent India in various Technical Commissions of International Institute of Welding. We assure continued support to IIW-INDIA in its efforts to put India in the world map of Welding Science and Technology.

ACKNOWLEDGEMENT

The help rendered by my colleague Dr. Shaju K. Albert, towards preparation of this paper is gratefully acknowledged. I am sincerely thankful to many of my present and former colleagues, including Mr. S. Murugan, Dr. M. Vasudevan, Dr. Anish Kumar, Dr. P. Palanichamy, Dr. B. P. C. Rao, Mrs. B. Sasi, Dr. B. Venkatraman, Dr. G. Sasikala, Dr. A. K. Bhaduri, Shri K. V. Kasiviswanathan and Dr. Hasan Shaikh for their valuable contributions.

REFERENCES

1. "The Use of Chromium and Nickel Equivalents in Considering Solidification Phenomena in Austenitic Stainless Steels" by N. Suutala and T. Moisio, in Solidification Technology in the Foundry and Cast-house, The Metals Society preprint, London, 1980.
2. "Feasibility studies on welding of D9I (IFAC-1 SS) tubes with SS 316 LN end plugs" - K. A. Gopal, S. Murugan, M.

Nandagopal, M. D. Mathew, G. Srinivasan, Shaju K. Albert, S. Venugopal, and T. Jayakumar Report no: IGC/MMG/IDEAS/D9I-316LN/1 dated Sept. 2011.

3. "A penetration enhancing flux formulation for tungsten inert gas (TIG) welding of austenitic stainless steels and its application" US Patent No. – WO 2008/056371 A1

4. P. Palanichamy, M. Vasudevan and T. Jayakumar, Measurement of Residual Stresses in Austenitic Stainless Steel Weld Joints using Ultrasonic Technique, Science and Technology of Welding and Joining, 14 (2), 2009, 166-171.

5. Sony Baby, K. V. Rajkumar, R. Subbaratnam, T. Balasubramanian, R. J. Pardikar, T. Jayakumar and Baldev Raj, Ultrasonic TOFD and SAFT for Evaluation of Flaws in Weldments – An Alternative to Radiography, Materials Evaluation, 64 (11), 2006, pp. 1089-1096.

6. Anish Kumar, K. Laha, T. Jayakumar, K. Bhanu Sankara Rao and Baldev Raj, Imaging of Modified 9Cr-1Mo Ferritic Steel Weldment by Ultrasonic Velocity Measurements, Science and Technology of Welding and Joining, 6, 2001, pp. 383-386.

7. G. S. Kumar et al. "Ultrasonic Imaging for Early Detection of Type-IV Cracking in Creep Tested Modified 9cr-1mo Ferritic Steel Weld Joints". Proceedings of "Review of Progress in Quantitative NDE", University of Vermont, July 17-22, 2011.

8. B. Venkatraman, T. Saravanan, T. Jayakumar, P. Kalyanasundaram and Baldev Raj, Assessment of Weld Joints of Steam Generator of PFBR by Microfocal Radiography, Canadian J. NDE, 25(4), July/Aug. 2004, pp. 6-13.

9. Baldev Raj and T. Jayakumar, Trends in Advanced Non-destructive Evaluation Techniques for Comprehensive Assessment of Engineering Materials and Components, J. Inst. Engineers (India), 80, 1999, pp.1-23.

10. C. Babu Rao, Raphaele Raillon, G.K. Sharma, T. Jayakumar, Philippe Benoist and Baldev Raj, Development of Inspection Modality for Shell Weld of Core Support Structure of a Fast Breeder Reactor Using CIA, Review of Quantitative Nondestructive Evaluation, American Inst. of Physics 29, 2010, pp. 1159-1166.

11. Hasan Shaikh, N. Sivaibharasi, B. Sasi, T. Anita, R. Amirthalingam, B.P.C. Rao, T. Jayakumar, H. S. Khatak and Baldev Raj, Use of Eddy Current Testing method in Detection and Evaluation of Sensitisation and Intergranular Corrosion in Austenitic Stainless Steels, Corrosion Science, 48, 2006, pp. 1462-1482.

12. M. Nani Babu et al. "Use of acoustic emission technique in fatigue crack growth characterisation" Proceedings of "Int. conference on creep, fatigue and creep fatigue interactions (CF-6)", Mahabalipuram, India, January 2012.

13. K. N. Gowtham, M. Vasudevan, V. Maduraimuthu and T. Jayakumar, Intelligent Modeling Combining Adaptive Neuro Fuzzy Inference System for Optimizing Welding Process Parameters, The minerals, Metals & Materials Society and ASM International 2011, 42 (2), 2011, pp. 385-392.

14. G. Srinivasan et al. "Development of filler wires for welding of reduced activation ferritic martenstic steel for India's test blanket module of ITER" Fusion Engineering Design, Volume 86, Issues 4–5, June 2011, Pages 446–451

15. N. Raghu et al, "Failure analysis of Dissimilar weld Failure on a steam pipeline Reducer", Proceedings-International Symposium on Material Ageing and Life Management (ISOMALM), IGCAR, Kalpakkam, Oct 3-6, 2000